

# NJC

Accepted Manuscript



This is an *Accepted Manuscript*, which has been through the Royal Society of Chemistry peer review process and has been accepted for publication.

*Accepted Manuscripts* are published online shortly after acceptance, before technical editing, formatting and proof reading. Using this free service, authors can make their results available to the community, in citable form, before we publish the edited article. We will replace this *Accepted Manuscript* with the edited and formatted *Advance Article* as soon as it is available.

You can find more information about *Accepted Manuscripts* in the [Information for Authors](#).

Please note that technical editing may introduce minor changes to the text and/or graphics, which may alter content. The journal's standard [Terms & Conditions](#) and the [Ethical guidelines](#) still apply. In no event shall the Royal Society of Chemistry be held responsible for any errors or omissions in this *Accepted Manuscript* or any consequences arising from the use of any information it contains.



Journal Name

COMMUNICATION

## Polyoxometalate-assisted fabrication of Pd nanoparticles/reduced graphene oxide nanocomposite with enhanced methanol-tolerance for the oxygen reduction reaction

Received 00th January 20xx,  
Accepted 00th January 20xx

DOI: 10.1039/x0xx00000x

www.rsc.org/

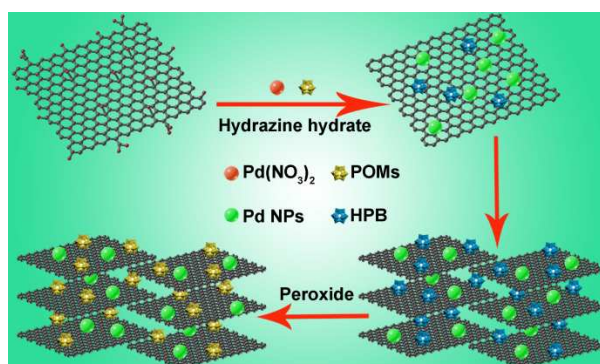
Ji-Sen Li,<sup>a,b</sup> Hui-Qing Dong,<sup>b</sup> Shun-Li Li,<sup>b</sup> Run-Han Li,<sup>b</sup> Zhi-Hui Dai,<sup>b\*</sup> Jian-Chun Bao,<sup>b</sup> and Ya-Qian Lan<sup>b\*</sup>

**A polyoxometalate (POM)-assisted fabrication of Pd nanoparticles/reduced graphene oxide (rGO) nanocomposite is reported. The hybrid exhibits enhanced catalytic activity and excellent methanol-tolerant capacity than its counterparts, due to the synergistic effect of Pd, POM, and rGO.**

In recent years, direct methanol fuel cells (DMFCs), as a class of proton exchange membrane fuel cells, have received considerable attention for energy storage and conversion due to their unique properties such as high power density, low to zero emissions and simple processing.<sup>1</sup> Nevertheless, there are some problems still preventing the commercialization of DMFCs, including the sluggish kinetics, high cost of Pt or Pt-based catalysts for oxygen reduction reaction (ORR) at the cathode, and methanol crossover through the membrane.<sup>2</sup> Hence, it is an urgent need to search for novel catalysts with lower cost, high efficiency, and excellent methanol-tolerance.

In this regard, Pd-based catalysts,<sup>3</sup> as promising alternatives, have been the focus of recent research for ORR, because they have relatively high electrocatalytic activity, even comparable to that of Pt-C catalyst, but their cost are lower than that of Pt-C. In addition, to further improve the catalytic performance of Pd nanoparticles (Pd NPs), a suitable support for the dispersy of Pd NPs is expected to exploit. Reduced graphene oxide (rGO), as a new support material, has been actively investigated because of its excellent electron transport property, and chemical stability.<sup>4</sup> But they are usually aggregated due to strong  $\pi$ -stacking and hydrophobic interactions, which impede the practical applications.<sup>5</sup> In parallel, polyoxometalates (POMs),<sup>6</sup> consisted of oxygen and transition-metal atoms, have attracted much interest due to their versatile physical and chemical properties, which are applied for catalysis, electrochemistry, energy storage, and so on. However, their

applications are immensely limited because of their lower surface area, and higher solubility in aqueous solution. Fortunately, due to the chemisorption interaction between carbon materials and POMs,<sup>7</sup> the POMs/rGO hybrid not only may overcome the above-mentioned shortcomings of POMs and rGO, but also significantly improve the electrocatalytic activity.<sup>8</sup> Inspired by the merit of Pd NPs, and POMs/rGO hybrid, we speculate that a novel metal nanoparticles/POMs/rGO composite is promising to be synthesized, which may further improve its electrocatalytic activity, and methanol-tolerance capacity. To date, to the best of our knowledge, only a limited number of metal nanoparticles/POMs/carbon composites as catalysts have been reported.<sup>9</sup> But the synthesis and application of porous Pd/POMs/rGO composite by assistance of POMs have not been explored for ORR so far. Therefore, it is a challenging task to fabricate novel Pd/POMs/rGO hybrid as an excellent electrocatalyst for ORR in DMFCs.



**Scheme 1** Preparation procedure of novel Pd/PMo12/rGO composite. HPB: heteropoly blue.

Herein, for the first time, we report a POM-assisted fabrication of Pd/PMo12/rGO nanocomposite using Pd(NO<sub>3</sub>)<sub>2</sub>, phosphomolybdic acid (PMo12), and graphene oxide as precursors (Scheme 1), which was served as a electrocatalyst for ORR in acid medium. The influence of the contents of Pd on the ORR was systematically investigated. The catalytic activity of Pd/PMo12/rGO is higher than its counterparts. Most importantly, the composite

<sup>a</sup> Key Laboratory of Inorganic Chemistry in Universities of Shandong, Department of Chemistry and Chemical Engineering, Jining University, Qufu, 273155, Shandong, P. R. China.

<sup>b</sup> Jiangsu Key Laboratory of Biofunctional Materials, College of Chemistry and Materials Science, Nanjing Normal University, Nanjing 210023, P. R. China E-mail: yqlan@njnu.edu.cn, daizhihui@njnu.edu.cn

Electronic Supplementary Information (ESI) available: [Experimental section, and additional figures and table]. See DOI: 10.1039/x0xx00000x

possesses outstanding methanol-tolerance, which is important for practical applications of DMFCs.

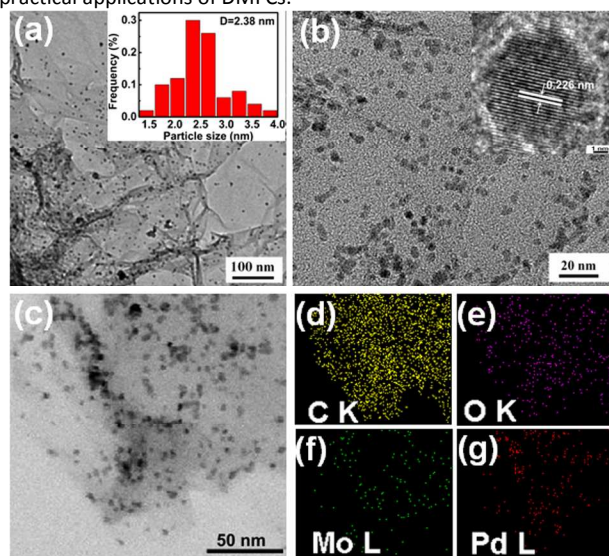


**Fig. 1** (a-c) TEM images of Pd/PMo12/rGO with different magnifications. Inset of (b): HRTEM image of Pd NP. Element-mapping images of Pd/PMo12/rGO (d) C, (e) O, (f) Mo, and (g) Pd.

The transmission electron microscopy (TEM) images of the Pd/PMo12/rGO composite with different magnifications are shown in Fig. 1a-c. The Pd NPs are uniformly dispersed or decorated on the wrinkled surfaces of rGO. By statistic analysis (inset of Fig. 1a), the average size of Pd is about 2.38 nm. The high-resolution TEM (HRTEM) image (inset of Fig. 1b) reveals that the fringe spacing of Pd is 0.226 nm. These results show that the agglomeration of Pd NPs was efficiently prevented due to the electrostatic repulsive interactions derived by PMo12 anions.<sup>9c, 10</sup> In addition, from element-mapping images (Fig. 1 d-g), the C, O, Mo, and Pd elements could be obviously observed, which efficiently attest the existence of Pd, PMo12, and rGO in the composite.

The structures of the composite were further characterized by the powder X-Ray diffraction (XRD), N<sub>2</sub> adsorption-desorption, fourier transform infrared spectrum (FTIR), and Raman spectrum. As shown in Fig. S1a (ESI<sup>†</sup>), the weak and broad peak at about 24° is observed, indicating that GO has been successfully reduced into rGO.<sup>9f, 11</sup> The characteristic peaks at 40.2, 46.7, 68.4, 82.4, and 87° are indexed to the (111) (200) (220) (311), and (222) planes of face-centered cubic Pd crystals (JCPDS-87-639). However, there are no noticeable diffraction peaks of PMo12, implying that PMo12 do not exist in the crystalline state, but in the dispersed state with no agglomeration.<sup>9c, 12</sup>

Fig. S1b (ESI<sup>†</sup>) reveals that the N<sub>2</sub> adsorption-desorption isotherms and corresponding pore size distributions of Pd/PMo12/rGO, and PMo12/rGO, which are of type IV with distinct hysteresis loops, implying a micro/mesoporous structure. Compared to those of the reported GO,<sup>13</sup> rGO,<sup>14</sup> and POMs,<sup>15</sup> the surface area of porous PMo12/rGO (488 m<sup>2</sup> g<sup>-1</sup>) increases, suggesting that the successful introduction of POMs breaks the face-to-face stacking of rGO nanosheets.<sup>12, 15</sup> Nevertheless, because the pores of PMo12/rGO are occupied by Pd NPs, the surface area

of Pd/PMo12/rGO (275 m<sup>2</sup> g<sup>-1</sup>) is lower than PMo12/rGO.<sup>9b</sup> The pore size distributions of PMo12/rGO, and Pd/PMo12/rGO are mainly centered at 3.8 nm on the basis of Barret-Joyner-Halenda (BJH) method, which are beneficial to promoting the diffusion of O<sub>2</sub>. As seen from FTIR spectra (Fig. S1c, and Fig. S2, ESI<sup>†</sup>), the characteristic peaks of PMo12 remain almost unchanged, demonstrating that PMo12 in the Pd/PMo12/rGO composite preserves its keggin structure. Whereas, the band of P=O of Pd/PMo12/rGO shifts to higher wavenumbers attributed to the interactions of Pd NPs and PMo12/rGO.<sup>9f, 15</sup> The detailed data were summarized in Table S1 (ESI<sup>†</sup>). In the Raman spectra (Fig. S1d, ESI<sup>†</sup>), it is found that the I<sub>D</sub>/I<sub>G</sub> values of Pd/PMo12/rGO, and PMo12/rGO are higher than that of GO, revealing more defects existing in the corresponding samples.<sup>9a</sup>

The electrocatalytic performance of Pd/PMo12/rGO for ORR was examined in a 0.1 M HClO<sub>4</sub> solution. As shown in Fig. 2a, the cathodic current density in an O<sub>2</sub>-saturated 0.1 M HClO<sub>4</sub> solution obviously increases in comparison with that in a N<sub>2</sub>-saturated solution, exhibiting an admirable electrocatalytic activity. To further assess the ORR process of the composite, linear sweep voltammograms (LSVs) were performed on a rotating-disk electrode (RDE) at a scan rate of 10 mV s<sup>-1</sup> and different rotating speeds from 100 to 2500 rpm in O<sub>2</sub>-saturated 0.1 M HClO<sub>4</sub> solution. Fig. 2b shows that the current density gradually increases with the rotating rate increasing because the diffusion rates of electrolytes are accelerated. The onset potential of Pd/PMo12/rGO for the ORR is approximately at 0.6 V vs Ag/AgCl electrode. Additionally, the corresponding Koutecky–Levich (K–L) plots and the electron transfer numbers for the ORR at different potentials are exhibited in Fig. 2c. The good linearity of K–L plots verifies first-order reaction kinetics for the ORR. According to the K–L equation (Experiment Section), the average electron transfer number (*n*) was calculated as about 3. Meanwhile, we carried out rotating ring-disk electrode (RRDE) measurement to investigate the ORR catalytic pathways of Pd/PMo12/rGO and Pt-C. It is found that the values of *n* for Pd/PMo12/rGO and Pt-C catalysts are 3 and 3.98, respectively (Fig. S3 (ESI<sup>†</sup>)), implying that the Pd/PMo12/rGO involves “2e<sup>-</sup> + 2e<sup>-</sup>” pathway for the ORR, with H<sub>2</sub>O<sub>2</sub> as the intermediate.<sup>16</sup> It is worth noting that, although the onset potential of Pd/PMo12/rGO is similar to those of PMo12/rGO, and Pd/rGO, the current density of Pd/PMo12/rGO is higher than PMo12/rGO, and Pd/rGO (Fig. 2d) due to the synergistic effect of Pd, PMo12, and rGO, which is slightly lower than commercial Pt-C. Thus, these results efficiently confirm that the Pd/PMo12/rGO catalyst is a promising alternative for ORR in the future.

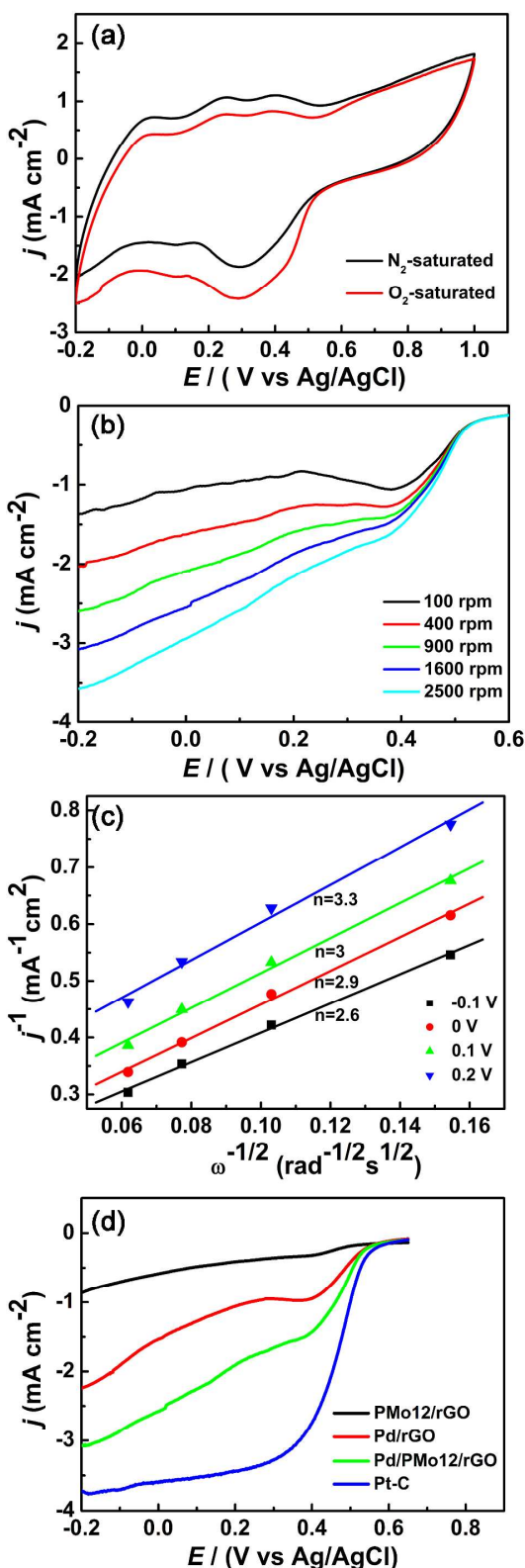


Fig. 2 (a) CVs of Pd/PMo12/rGO in a  $N_2$  or  $O_2$ -saturated 0.1 M  $HClO_4$  solution; (b) LSVs of Pd/PMo12/rGO at various rotation rates; (c) K-L plots of Pd/PMo12/rGO at various potential; (d) LSVs of different samples at a rotation rate of 1600 rpm.

In control experiment, to illustrate the effect of the contents of Pd on the ORR activity, the composites contained different contents of Pd NPs were synthesized, denoted as Pd/PMo12/rGO (X) (where X stands for the contents of  $Pd(NO_3)_2$ ). From Fig. S4 (ESI<sup>†</sup>), although the contents of Pd NPs are increased, the onset potential remains unchanged. On contrast, compared to Pd/PMo12/rGO, due to few active species observed from Fig. S5a (ESI<sup>†</sup>), the Pd/PMo12/rGO (30) catalyst shows slightly lower limiting current density. As for Pd/PMo12/rGO (100), with the increase of the content of  $Pd(NO_3)_2$ , the Pd NPs were agglomerated into bigger particles (Fig. S5b, ESI<sup>†</sup>), further decreasing the limiting current density. Thus, it is worthwhile noting that the contents of Pd might be one of the most important issues for the electrocatalytic properties of Pd/PMo12/rGO.

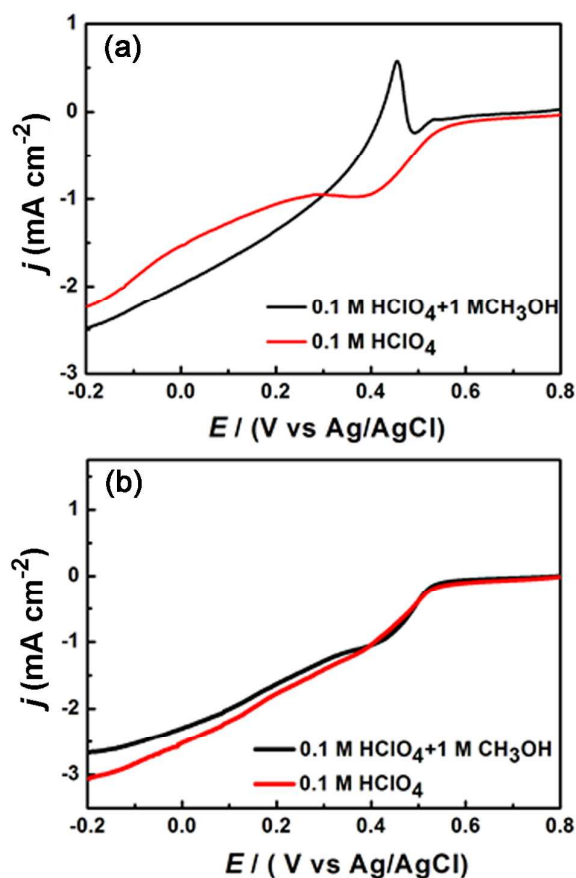


Fig. 3 LSVs of Pd/rGO (a), and Pd/PMo12/rGO (b) in  $O_2$ -saturated 0.1 M  $HClO_4$  solutions upon addition of methanol at a rotation rate of 1600 rpm.

In addition, the methanol-tolerance capacity is an important parameter for the practical applications of DMFCs. As shown in Fig. 3a and S6 (ESI<sup>†</sup>), there are noticed ORR signals of Pd/rGO, and Pt-C catalysts in LSVs when methanol is added into an  $O_2$ -saturated 0.1 M  $HClO_4$  solution at a rotation rate of 1600 rpm. On the contrary, for Pd/PMo12/rGO, it is found that the two LSVs almost completely overlap (Fig. 3b), demonstrating that the Pd/PMo12/rGO catalyst has an excellent tolerance to the methanol cross-over effect,

superior to that of the commercial Pt-C catalyst, which is very important for practical applications of DMFCs.

Considering the above results, the predominant electrocatalytic activity and methanol-tolerance of Pd/PMo12/rGO may originate from the following key aspects. (1) rGO, as a support, may boost electronic conductivity and mass transfer.<sup>17</sup> As well, the introduction of well-distributed Pd NPs with small sizes increases the active species, further improving catalytic capacity.<sup>9h</sup> (2) The porous structures and large surface area, stemming from the interactions of PMo12 and rGO, provide much more sites to uniformly disperse Pd nanoparticles, accessible paths for the approach of O<sub>2</sub> to active sites and simultaneously hinder the contact of methanol and activity sites.<sup>2b</sup> Moreover, PMo12 with high ionic conductivity may be helpful for the capture of oxygen, and water molecules, and the dispersibility of rGO.<sup>9b</sup> (3) a synergistic effect of Pd, PMo12, and rGO is beneficial to the above-mentioned performance.

In summary, a novel Pd/PMo12/rGO nanocomposition was prepared by assistance of PMo12. The structure of the hybrid was characterized in detail, further confirming the successful fabrication of Pd/PMo12/rGO. Pd NPs, as active species, were uniformly distributed over the surfaces of rGO. Porous structures and high ionic conductivity, originating from the interactions of PMo12 and rGO, are beneficial for promoting the diffusion of reactant. Taking advantage of these merits, the composite exhibits better electrocatalytic performance and outstanding methanol-tolerance capacity. The work opens up exciting opportunities for developing multicomponent electrocatalysts as promising candidates for DMFCs.

## Experimental

### Synthesis of Pd/PMo12/rGO

60 mg of GO was dispersed in 20 mL double-distilled H<sub>2</sub>O to form a homogeneous suspension by ultrasonication. And then, 20 mL Pd(NO<sub>3</sub>)<sub>2</sub> solution (3 mg L<sup>-1</sup>) was added into the above solution followed by ultrasonication for 30 min. During the process, the brown-colored product appeared. Subsequently, 20 mL PMo12 solution (5 mM) and 20 mL double-distilled H<sub>2</sub>O were added into above solution followed by ultrasonication for 30 min at 30 - 40 °C. Hydrazine hydrate (1 mL, 80 wt%) was added into the mixture. The solution became black immediately. After 2 h, large particles or solids floating on the liquid surface were obtained, and PMo12 was converted into heteropoly blue (HPB). And then, all solids were centrifuged and washed with water and ethanol to remove byproducts, and dried in vacuum at 40 °C for 12 h (denoted as Pd/HPB/rGO). The obtained composite was dispersed in 40 mL double-distilled H<sub>2</sub>O, further added 13 mL solution (10 mL H<sub>2</sub>O + 3 mL H<sub>2</sub>O<sub>2</sub>) and vigorous stirring for 2 h, followed by keeping quiescent for another 12 h. The sample was collected by the above procedures which are similar to that for HPB/rGO (defined as Pd/PMo12/rGO).

## Acknowledgements

This work was financially supported by the NSFC (No. 21371099, 21471080, and 21475062), the program of Jiangsu Specially-Appointed Professor, the NSF of Jiangsu Province of China (No. BK20130043), the Natural Science Research of Jiangsu Higher Education Institutions of China (No. 13KJB150021), the Priority Academic Program Development of Jiangsu Higher Education Institutions, the Natural Science Foundation of Shandong Province (No. ZR2014BQ037), and the Youths Science Foundation of Jining University (No. 2014QNKJ08).

## Notes and references

- (a) Y. J. Wang, D. P. Wilkinson, J. Zhang, *Chem. Rev.* 2011, **111**, 7625; (b) X. Zhao, M. Yin, L. Ma, L. Liang, C. Liu, J. Liao, T. Lu, W. Xing, *Energy Environ. Sci.* 2011, **4**, 2736.
- (a) X. Huang, Z. Zhao, Y. Chen, E. Zhu, M. Li, X. Duan, Y. Huang, *Energy Environ. Sci.* 2014, **7**, 2957; (b) Z. Wen, J. Liu, J. Li, *Adv. Mater.* 2008, **20**, 743; (c) E. Antolini, *ChemPlusChem* 2014, **79**, 765.
- (a) C. Bianchini, P. K. Shen, *Chem. Rev.* 2009, **109**, 4183; (b) L. Xiao, L. Zhuang, Y. Liu, J. Lu, H. D. Abruña, *J. Am. Chem. Soc.* 2008, **131**, 602; (c) M.-H. Shao, K. Sasaki, R. R. Adzic, *J. Am. Chem. Soc.* 2006, **128**, 3526.
- (a) D. A. C. Brownson, D. K. Kampouris, C. E. Banks, *Chem. Soc. Rev.* 2012, **41**, 6944; (b) H. Li, S. Pang, S. Wu, X. Feng, K. Müllen, C. Bubeck, *J. Am. Chem. Soc.* 2011, **133**, 9423; (c) D. R. Dreyer, S. Park, C. W. Bielawski, R. S. Ruoff, *Chem. Soc. Rev.* 2010, **39**, 228.
- (a) P. V. Kamat, *J. Phys. Chem. Lett.* 2009, **1**, 520; (b) C. Huang, C. Li, G. Shi, *Energy Environ. Sci.* 2012, **5**, 8848.
- (a) L. Cronin, A. Muller, *Chem. Soc. Rev.* 2012, **41**, 7333; (b) D.-Y. Du, J.-S. Qin, S.-L. Li, Z.-M. Su, Y.-Q. Lan, *Chem. Soc. Rev.* 2014, **43**, 4615; (c) D.-L. Long, R. Tsunashima, L. Cronin, D.-L. Long, R. Tsunashima, L. Cronin, *Angew. Chem. Int. Ed.* 2010, **49**, 1736; (d) M. Ammam, *J. Mater. Chem. A* 2013, **1**, 6291.
- Z. Kang, Y. Liu, C. H. A. Tsang, D. D. D. Ma, E. Wang, S.-T. Lee, *Chem. Commun.* 2009, **4**, 413.
- (a) S.-X. Guo, Y. Liu, C.-Y. Lee, A. M. Bond, J. Zhang, Y. V. Geletii, C. L. Hill, *Energy Environ. Sci.* 2013, **6**, 2654; (b) M. Jiang, D. Zhu, J. Cai, H. Zhang, X. Zhao, *J. Phys. Chem. C* 2014, **118**, 14371; (c) B. Xia, Y. Yan, X. Wang and X. W. Lou, *Mater. Horiz.* 2014, **1**, 379.
- (a) R. Liu, S. Li, X. Yu, G. Zhang, S. Zhang, J. Yao, B. Keita, L. Nadjo, L. Zhi, *Small* 2012, **8**, 1398; (b) H. Liu, Y. Zheng, G. Wang, S. Z. Qiao, *Adv. Energy Mater.* 2015, **5**, 1401186; (c) X. Zhao, J. Zhu, L. Liang, C. Liu, J. Liao, W. Xing, *J. Power Sources* 2012, **210**, 392; (d) Y. Ji, L. Shen, A. Wang, M. Wu, Y. Tang, Y. Chen, T. Lu, *J. Power Sources* 2014, **260**, 82; (e) R. Liu, S. Li, X. Yu, G. Zhang, Y. Ma, J. Yao, *J. Mater. Chem.* 2011, **21**, 14917; (f) R. Liu, X. Yu, G. Zhang, S. Zhang, H. Cao, A. Dolbecq, P. Mialane, B. Keita, L. Zhi, *J. Mater. Chem. A* 2013, **1**, 11961; (g) S. Li, X. Yu, G. Zhang, Y. Ma, J. Yao, P. de Oliveira, *Carbon* 2011, **49**, 1906; (h) R. Liu, S. Li, X. Yu, G. Zhang, S. Zhang, J. Yao, L. Zhi, *J. Mater. Chem.* 2012, **22**, 3319.
- S. Özkar, R. G. Finke, *J. Am. Chem. Soc.* 2002, **124**, 5796.
- G. H. Jeong, S. H. Kim, M. Kim, D. Choi, J. H. Lee, J.-H. Kim, S.-W. Kim, *Chem. Commun.* 2011, **47**, 12236.
- S. Wang, H. Li, S. Li, F. Liu, D. Wu, X. Feng, L. Wu, *Chem. Eur. J.* 2013, **19**, 10895.
- D.-D. Zhang, S.-Z. Zu, B.-H. Han, *Carbon* 2009, **47**, 2993.
- Y. Si, E. T. Samulski, *Chem. Mater.* 2008, **20**, 6792.
- D. Zhou, B.-H. Han, *Adv. Func. Mater.* 2010, **20**, 2717.
- P. S. Ruvinskiy, A. Bonnefont, C. Pham-Huu, E. R. Savinova, *Langmuir* 2011, **27**, 9018.
- C. N. R. Rao, H. S. S. R. Matte, K. S. Subrahmanyam, *Acc. Chem. Res.* 2012, **46**, 149.

## Graphical abstract

### Polyoxometalate-assisted fabrication of Pd nanoparticles/reduced graphene oxide nanocomposite with enhanced methanol-tolerance for the oxygen reduction reaction

Ji-Sen Li,<sup>a,b</sup> Hui-Qing Dong,<sup>b</sup> Shun-Li Li,<sup>b</sup> Run-Han Li,<sup>b</sup> Zhi-Hui Dai,<sup>b\*</sup> Jian-Chun Bao,<sup>b</sup> and Ya-Qian Lan<sup>b\*</sup>

The prepared Pd/polyoxometalate/reduced graphene oxide (Pd/POM/rGO) nanocomposite exhibits enhanced catalytic activity and excellent methanol-tolerance due to the synergistic effect of Pd, POM, and rGO.

